

Dihedral Tilings of the Sphere by Regular Polygons and Quadrilaterals II: Regular Polygons with High Gonality and Rhombi

Ho Man CHEUNG¹ and Hoi Ping LUK²

²The Hong Kong University of Science & Technology

¹email: hmcheungae@connect.ust.hk

²email: hoi@connect.ust.hk

March 13, 2024

Abstract

We classify the dihedral edge-to-edge tilings of the sphere by regular polygons with gonality $m \geq 5$ and rhombi.

Keywords: Classification, Spherical tilings, Dihedral tilings, Spherical polygons, Division of spaces

Mathematics Subject Classification: 05B45, 52C20, 51M09, 51M20

1 Introduction

This paper is the second of the series to classify dihedral tilings of the sphere, where one prototile is a regular polygon and the other is a rhombus. The two prototiles in the first [12] of the series are one square and one rhombus. The two prototiles in this paper are one regular polygon (m -gon with $m \geq 5$ and edge combination x^m and angles α) and one rhombus (with edge combination x^4 and angles β, γ). The prototiles are illustrated in Figure 1 where the regular polygon is shaded and the rhombus is unshaded. Throughout this paper, the shaded tiles are always regular m -gons. We assume that the degree of a vertex is ≥ 3 .

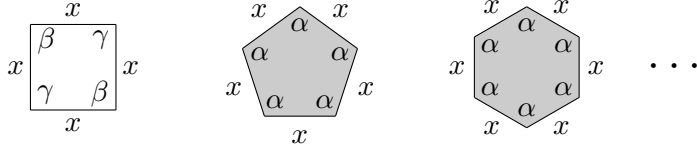


Figure 1: Rhombus and regular polygons

The main result is given below, where f denotes the number of tiles.

Theorem. *The dihedral tilings of the sphere by regular polygons with gonality $m \geq 5$ and rhombi are*

- I. *Earth map type: one infinite family of tilings with $f = 8c - 2$, where $c \geq 2$ and $m = 5$, and vertices $\{\beta^2\gamma, \alpha\beta\gamma^c\}$;*
- II. *Prism type: one infinite family of tilings with $f = m + 2$, and vertex $\{\alpha\beta\gamma\}$;*
- III. *Archimedean type:*
 - *three triangular fusions of the snub dodecahedron with $m = 5$, and $f = 52$, and vertices $\{\alpha\beta^2, \alpha\beta\gamma^2\}$;*
 - *one quadrilateral subdivision of the truncated icosahedron with $m = 5$, $f = 72$, and vertices $\{\beta^3, \alpha\beta\gamma^2\}$.*

The family of earth map type are derived from the monohedral tilings $E_{\square}4$ in [8]. The first picture of Figure 2 shows a part of $E_{\square}4$ with γ^3 at one end and γ^2 at the other. Let \mathcal{T} denote the general version of it consisting of $2c - 1$ rhombi with γ^c at one end and γ^{c-1} at the other (the first picture shows $c = 3$). The earth map type tilings are constructed by four copies of \mathcal{T} and 2 regular pentagons. The four \mathcal{T} 's are glued together between the two pentagons as illustrated in the second picture.

The family of prism type are derived from prisms with two congruent m -gons on top and at the bottom and the cylindrical middle consists of m rhombi. We remark that the corresponding tilings with the regular m -gon as regular triangle or square respectively also belong to the same family in Figure 3.

The tilings of Archimedean type in Figure 4. The first three tilings are triangular fusions of the snub dodecahedron and the fourth one is a quadrilateral subdivision of a (deformed) truncated icosahedron (or commonly known as the Adidas Telstar football).

The three triangular fusions of the snub dodecahedron are explained in Figure 5. The first picture illustrates the snub dodecahedron, which is a dihedral tiling of the

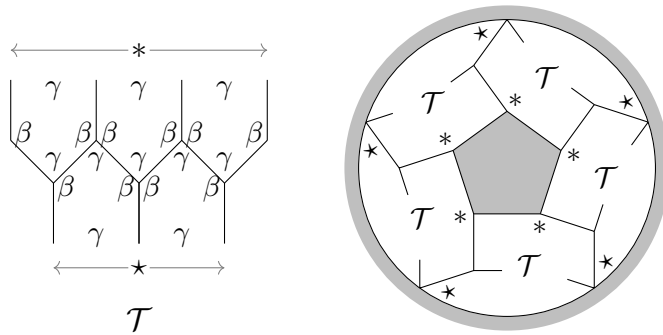


Figure 2: The earth map type, an infinite family of tilings with $\beta^2\gamma, \alpha\beta\gamma^c$

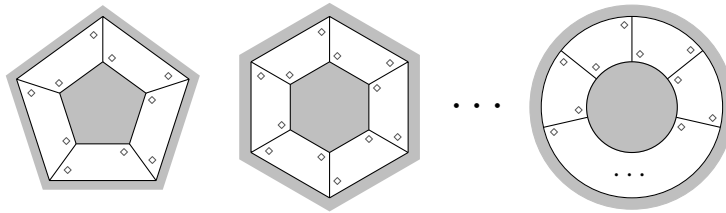


Figure 3: The earth map type: prisms consist of two regular m -gons and m rhombi, $m \geq 5$ and $\diamond = \beta$

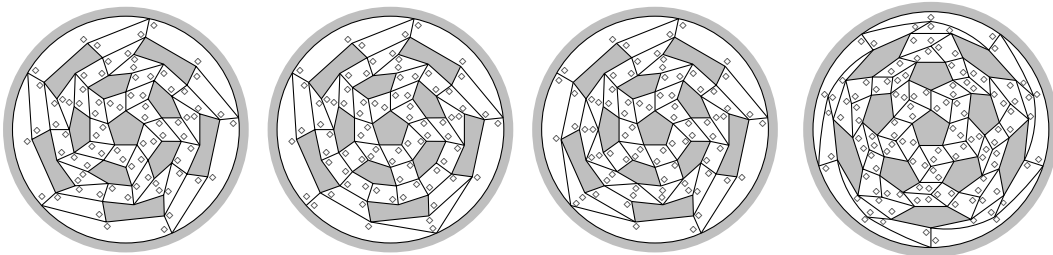


Figure 4: The four Archimedean type tilings, by regular pentagons and rhombi, $\diamond = \beta$

sphere by regular triangles and regular pentagons. In general, if the triangles in a dihedral tiling can be grouped into adjacent pairs, then by fusing all the pairs we get quadrilaterals. In the snub dodecahedron, all triangles are regular. Therefore the fusion gives congruent rhombi. The dashed line in Figure 5 represent the choice of adjacent pairs. The second, third and fourth picture are all possible ways to group the pairs.

To distinguish the last three tilings in Figure 5, we denote the vertices at the

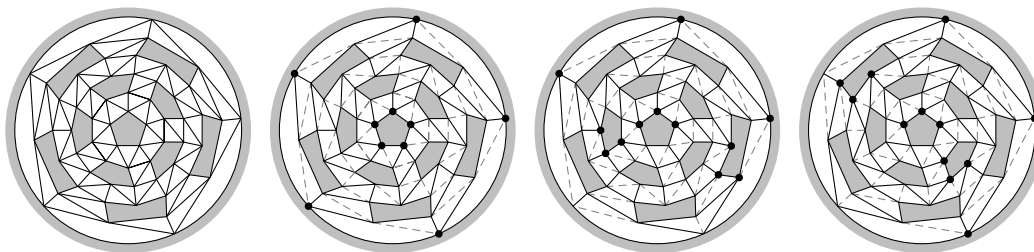


Figure 5: Three triangular fusions of the snub dodecahedron

pentagons with exterior edge configuration “dashed-solid-solid” by \bullet 's. To highlight the difference, we only display them at pentagons with at least three such vertices. The distribution of \bullet 's shows that the the second tiling is different from the third and the fourth in Figure 5. The third and the fourth tiling are differentiated in Figure 6. We look at the (shortest) path through rhombi from the middle \bullet of a trio to the opposite edge to a middle \bullet of another trio. In the left picture, from the trio at the centre pentagon to the specified edge of its immediate neighbouring pentagon, the path goes through three rhombi. In the right picture, the corresponding path goes through two rhombi.

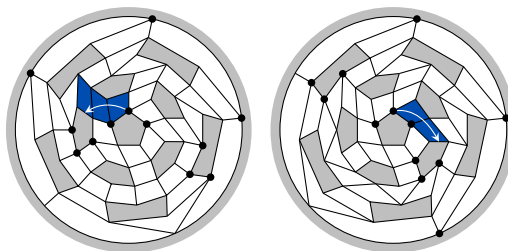


Figure 6: Difference between two triangular fusions of the snub dodecahedron

It is interesting to note that, the three triangular fusions of the snub dodecahedron can also be derived from the 1-factors of the graph of dodecahedron. The explanation of such connection can be seen at the end of the proof of Proposition 3.5.

The fourth tiling in Figure 4 can be derived from a truncated icosahedron. Each hexagon in Figure 7 is divided into three kites (by red dotted lines), and form a one parameter family of tiling with regular pentagon and kite. For one special value, the kite becomes rhombus.

Throughout this paper, a pentagon refers to a regular pentagon and an m -gon refers to a regular m -gon with $m \geq 6$ unless otherwise specified.

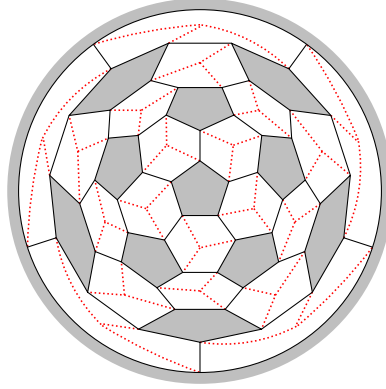


Figure 7: A quadrilateral subdivision of the truncated icosahedron (football)

This paper is organised as follows. In Section 2, we explain the basic terminology and tools. In Section 3, we classify the tilings by pentagons and rhombi. In Section 4, we classify the tilings by m -gons with $m \geq 6$ and rhombi. The key to classification is to find all the vertices in the tilings. The sporadic tilings are obtained in Propositions 3.4, 3.5. The first infinite family is obtained in Proposition 3.7 and the second infinite family is obtained in Propositions 3.1, 4.3.

2 Basics

The *vertex angle sum* of a vertex $\alpha^a\beta^b\gamma^c$, consisting of a copies of α and b copies of β and c copies of γ , is

$$a\alpha + b\beta + c\gamma = 2\pi. \quad (2.1)$$

In a vertex notation, a, b, c are assumed to be > 0 unless otherwise specified. That is, we only express the angles appearing at a vertex whenever possible. For example, $\alpha\beta^2$ is a vertex with $a = 1, b = 2$ and $c = 0$. The notation $\alpha\beta^2 \cdots$ means a vertex with at least one α and two β 's, i.e., $a \geq 1$ and $b \geq 2$. The angle combination in \cdots is called the *remainder* of the vertex. The value of the remainder is denoted by R . For example, $R(\alpha\beta^2) = 2\pi - \alpha - 2\beta$.

There are various constraints on the angle combinations at vertices in a tiling. Examples of such constraints are the vertex angle sum and the quadrilateral angle sum. A collection of all vertices in a tiling satisfying various constraints is called an *anglewise vertex combination* (AVC). The following AVC is from (3.3),

$$\text{AVC} = \{\beta^2\gamma, \beta\gamma^c, \alpha\beta\gamma^c\}.$$

The generic c may take different values at different vertex. The tilings constructed from (3.3) do not have $\beta\gamma^c$. We use “ \equiv ” in place of “ $=$ ” to denote the set of all vertices which actually appear in a tiling. For example, we have the following for the tilings in Figure 20

$$\text{AVC} \equiv \{\beta^2\gamma, \alpha\beta\gamma^c\}.$$

To obtain the vertices, it is necessary and convenient to have notations for studying various angle arrangements. For example, $\alpha_1\gamma_2\cdots$ denotes the vertex where T_1 contributes α and T_2 contributes γ in the first picture of Figure 8. To emphasize α_1 is adjacent to γ_2 along an edge “ $|$ ”, we use $\alpha_1|\gamma_2\cdots$ to denote the vertex. In addition, the same picture shows that $\alpha|\gamma\cdots$ is a vertex if and only if $\alpha|\beta\cdots$ is a vertex. Similarly, T_1, T_2 in the second picture of Figure 8 show that $\gamma|\gamma\cdots$ is a vertex if and only if $\beta|\beta\cdots$ is also a vertex. For a full vertex, such as α^3 in the third picture, we use $|\alpha|\alpha|\alpha|$ to denote its angle arrangement.

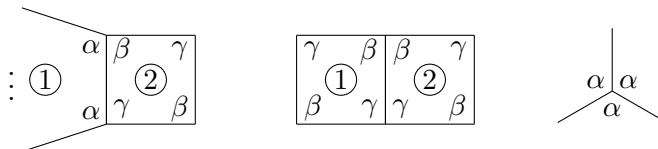


Figure 8: The arrangements of $\alpha|\gamma$ and $\gamma|\gamma$ and $\beta|\beta$ and α^3

The following lemma follows from a well-known fact on triangle-free graphs on the sphere with vertex degree ≥ 3 .

Lemma 2.1. *There is a degree 3 vertex in a dihedral tiling by quadrilaterals and m -gons where $m \geq 5$.*

Lemma 2.2 (Counting Lemma, [12, Lemma 2.3]). *In a dihedral tiling of the sphere by regular m -gons and rhombi, If at every vertex the number of β is no more than the number of γ , then at every vertex these two numbers are equal.*

The angle sum of the regular m -gon is $m\alpha > (m - 2)\pi$ and the rhombus angle sum is $2\beta + 2\gamma > 2\pi$. Then we get

$$\alpha > \left(1 - \frac{2}{m}\right)\pi, \quad \beta + \gamma > \pi.$$

Up to symmetry between β, γ , we may assume $\beta > \gamma$. This implies $\beta > \frac{1}{2}\pi$.

In a dihedral tiling by regular m -gons and rhombi, there is a pair of adjacent tiles consisted of one m -gon and one rhombus in the first picture of Figure 8. The next lemma follows from this observation.

Lemma 2.3. *In a dihedral tiling by regular m -gons and rhombi, $\alpha\beta\cdots, \alpha\gamma\cdots$ are vertices.*

An immediate consequence of Lemma 2.3 is that one of $\alpha^a\beta^b, \alpha\beta\gamma\cdots$ is a vertex. Then we have one of the inequalities, $2\alpha+\beta \leq 2\pi$ and $\alpha+2\beta \leq 2\pi$ and $\alpha+\beta+\gamma \leq 2\pi$. Combined with $\alpha > (1 - \frac{2}{m})\pi$ and $\beta > \gamma$ and $\beta + \gamma > \pi$, we know $\alpha, \gamma < \pi$. Hence the regular m -gon is convex.

By [7, Lemma 5.2] or [8, Lemma 18], we have

$$\cos x = \cot \frac{1}{2}\beta \cot \frac{1}{2}\gamma. \quad (2.2)$$

On the other hand, the spherical cosine law for angles on the regular m -gon implies

$$\cos x = \cot^2 \frac{1}{2}\alpha + \frac{\cos \frac{2}{m}\pi}{\sin^2 \frac{1}{2}\alpha}. \quad (2.3)$$

Combining the two identities, we get

$$\cot^2 \frac{1}{2}\alpha + \cos \frac{2}{m}\pi \csc^2 \frac{1}{2}\alpha = \cot \frac{1}{2}\beta \cot \frac{1}{2}\gamma, \quad (2.4)$$

Then for $m \geq 5$ and $\gamma \in (0, \pi)$, we get $\cot \frac{1}{2}\beta > 0$, which implies $\beta < \pi$. Meanwhile, by $m \geq 5$ and $\beta > \gamma$ and (2.4), we get $\cot \frac{1}{2}\beta \cot \frac{1}{2}\gamma > \cot^2 \frac{1}{2}\alpha$. By $\alpha, \beta, \gamma \in (0, \pi)$ and $\cot \theta$ is strictly decreasing on $(0, \pi)$, this implies $\alpha > \gamma$. So γ is the smallest angle. Hence we have $\alpha, \beta > \gamma$ throughout this paper.

By Lemma 2.1, there is a degree 3 vertex. By $\alpha\beta\cdots$, we have one of the inequalities $2\alpha + \beta \leq 2\pi$ and $\alpha + 2\beta \leq 2\pi$ and $\alpha + \beta + \gamma \leq 2\pi$. Then $\alpha, \beta > \gamma$ imply

$$\alpha + \beta + \gamma \leq 2\pi. \quad (2.5)$$

It further implies that $\gamma^3, \alpha\gamma^2, \beta\gamma^2$ are not vertices. For $\alpha^3, \beta^3, \alpha^2\beta, \alpha\beta^2$, the inequality $\beta \geq \alpha$ implies $\beta \geq \frac{2}{3}\pi \geq \alpha$. Combined with $\alpha > (1 - \frac{2}{m})\pi$, we get $m < 6$. This means that $\alpha^3, \beta^3, \alpha^2\beta, \alpha\beta^2$ are not vertices for m -gons with $m \geq 6$. Hence one of the following degree 3 vertices must appear in a dihedral tiling for the given gonality $m \geq 5$,

$$m = 5: \quad \alpha^3, \alpha^2\gamma, \beta^3, \alpha^2\beta, \alpha\beta^2, \beta^2\gamma, \alpha\beta\gamma; \quad (2.6)$$

$$m \geq 6: \quad \alpha^2\gamma, \beta^2\gamma, \alpha\beta\gamma. \quad (2.7)$$

3 Tilings by Rhombi and Pentagons

Proposition 3.1. *The dihedral tiling with vertex $\alpha\beta\gamma$ is in Figure 9.*

The tiling is given by the prism with 2 pentagons and 5 rhombi. The tiling is the first one in Figure 3.

We remark that $\alpha \geq \beta > \gamma$ implies $\alpha\beta\cdots = \alpha\beta\gamma$ for the following reason. If $\alpha \geq \beta$, then by $\beta + \gamma > \pi$ we get $R(\alpha\beta) \leq R(\beta^2) < 2\gamma$. By $\alpha, \beta > \gamma$, we have $\alpha\beta\cdots = \alpha\beta\gamma$. Since Lemma 2.3 implies that $\alpha\beta\cdots$ is a vertex, for the studies where $\alpha\beta\gamma$ is not a vertex, it suffices to consider $\beta > \alpha > \gamma$.

Proof. By $\alpha\beta\gamma$, we have $R(\alpha\beta) = \gamma$. Then by $\alpha, \beta > \gamma$, we get $\alpha\beta\cdots = \alpha\beta\gamma$. Meanwhile, by $\beta + \gamma > \pi$, we also have $R(\beta^2) < 2\gamma$. Then we get $\beta^2\cdots = \beta^3, \beta^2\gamma$.

By $\alpha\beta\cdots = \alpha\beta\gamma$ and $\beta^2\cdots = \beta^3, \beta^2\gamma$, we get $\beta\cdots = \alpha\beta\gamma, \beta^3, \beta^2\gamma, \beta\gamma^c$. The other vertices consist of only α, γ , which are $\alpha^a, \alpha^a\gamma^c, \gamma^c$. By $\alpha > \frac{3}{5}\pi$, we further get $\alpha^a = \alpha^3$. Hence we have the vertices below

$$\alpha^3, \beta^3, \beta^2\gamma, \alpha\beta\gamma, \gamma^c, \alpha^a\gamma^c, \beta\gamma^c.$$

The arrangement $\alpha|\gamma$ determines tiles T_1, T_2 in the first picture of Figure 9. Then $\alpha_1\beta_2\cdots = \alpha\beta\gamma$ determines T_3 . By the same argument, we further determine T_4, T_5, T_6 , which implies $\alpha|\gamma\cdots = \alpha\beta\gamma$. Then $\alpha^a\gamma^c$ is not a vertex and $\alpha^2\cdots = \alpha^3$.

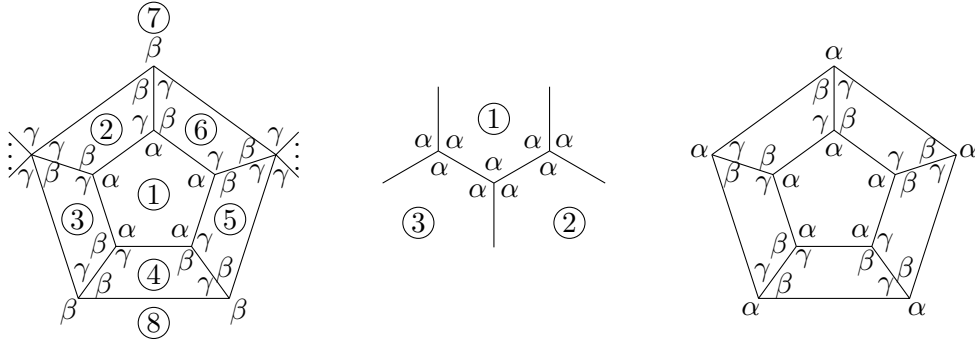


Figure 9: Construction of the tiling with $\alpha\beta\gamma$

By $\alpha^2\cdots = \alpha^3$, starting at an α^3 , we get tiles T_1, T_2, T_3 in the second picture of Figure 9 and the starting vertex is $\alpha_1\alpha_2\alpha_3$. Then by $\alpha^2\cdots = \alpha^3$, we also know the two adjacent vertices $\alpha_1\alpha_2\cdots, \alpha_1\alpha_3\cdots = \alpha^3$. Repeating this process, we determine a monohedral tiling given by the dodecahedron.

So α^3 is not a vertex of dihedral tiling and hence it remains to discuss the following,

$$\beta^3, \beta^2\gamma, \alpha\beta\gamma, \gamma^c, \beta\gamma^c.$$

Since α appears at some vertex, we know that $\alpha\beta\gamma$ is a vertex and $\alpha\beta\cdots = \alpha\gamma\cdots = \alpha\beta\gamma$.

Starting at an $\alpha\beta\gamma$, by $\alpha\beta\cdots = \alpha\gamma\cdots = \alpha\beta\gamma$ we determine T_1, T_2, \dots, T_6 in the first picture of Figure 9. If the undetermined $\beta_2\gamma_6\cdots = \beta^2\gamma$, then we determine T_7 . By $\beta_3\gamma_2\gamma_7\cdots, \beta_6\gamma_5\gamma_7\cdots = \beta\gamma^c$, we further determine T_8 with two adjacent β 's, a contradiction. This means that none of the undetermined $\beta|\gamma\cdots$ at T_2, \dots, T_6 is $\beta^2\gamma$. Hence they must be $\alpha\beta\gamma$. This determines a tiling in the third picture of Figure 9 with

$$\text{AVC} \equiv \{\alpha\beta\gamma\}.$$

We remark that $\beta^3, \beta^2\gamma, \gamma^c, \beta\gamma^c$ are not vertices for the dihedral tiling.

Geometric Realisation

It remains to show that the tiling exists. It suffices to show that for the two regular pentagons with edge length x placed equal distance (denoted by h) away from the equator in the north and south hemispheres respectively, one can subdivide the cylinder into five rhombi with length x .

Consider a lune defined by the north pole N and the south pole S and A_1, A_2, B_1, B_2 where the arcs A_1A_2, B_1B_2 have lengths x and A_1, A_2 (and respectively B_1, B_2) are equal distance from the equator (dotted line) in Figure 10, i.e., $NA_1 = NA_2 = SB_1 = SB_2 = r$ for some $r \in (0, \frac{1}{2}\pi)$. Then we have $h = \pi - 2r$.

Let $\lambda(A_1A_2)$ denote segment of latitude defined by A_1, A_2 . For $h < x$, we show that there is an $X_1 \in \lambda(A_1A_2)$ such that $B_1X_1 = x$. By $r < \frac{1}{2}\pi$, we have $\theta' < \frac{1}{2}\pi$ and therefore $\theta > \frac{1}{2}\pi$. For $h < x < \pi$ and $A_2B_1 < \pi$, the triangle $\triangle A_1A_2B_1$ is a standard triangle and hence $x > h$ implies $\psi > \phi$. Meanwhile, the arc A_2B_1 divides the lune into two identical halves. By the rotational symmetry of the subdivided lune, we know that $\psi < \frac{1}{2}\pi$. Then we have $\theta > \frac{1}{2}\pi > \psi > \phi$ and hence $A_2B_1 > x > h$. For $X \in \lambda(A_1, A_2)$, by $h = \pi - 2r$ and cosine law on $\triangle B_1NX$, we get $\cos B_1X = \cos(h+r)\cos r + \sin(h+r)\sin r \cos \xi = -\cos^2 r + \sin^2 r \cos \xi$. For each fixed r , the length of B_1X is a continuous function of ξ such that $B_1X = h$ when $\xi = 0$ and $B_1X = B_1A_2$ when $\xi = \frac{2}{m}\pi$ where $m = 5$. Intermediate Value Theorem implies that there is a point $X_1 \in \lambda(A_1A_2)$ (given by $\xi_1 \in (0, \frac{2}{m}\pi)$) such that $B_1X_1 = x$. By repeating the same process for each pair of vertices B_i, B_{i+1} for the pentagon in

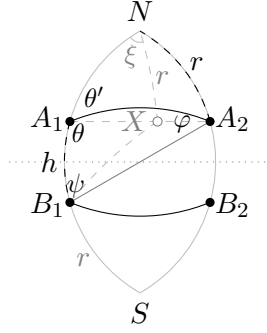


Figure 10: Geometric realisation of tiles

the lower hemisphere, we locate the vertices X_1, \dots, X_5 for the pentagon in the upper hemisphere and the rhombi are defined by edges $B_1X_1, B_2X_2, \dots, B_5X_5$. Since the interiors of each lune are disjoint, the B_iX_i 's do not intersect. Therefore we can in fact obtain simple rhombi.

Note that the same construction works for all regular polygons with gonality $m \geq 3$. Cosine law on $\triangle NA_1A_2$ gives $\cos x = \cos^2 r + \sin^2 r \cos \frac{2}{m}\pi$. For $\pi - 2r = h < x$, it further implies $r > \cot^{-1} \sin \frac{1}{m}\pi$. Hence for each m , the construction works for any choice of $r \in (\cot^{-1} \sin \frac{\pi}{m}, \frac{1}{2}\pi)$. \square

Proposition 3.2. *There is no dihedral tiling with vertex $\alpha^2\gamma$.*

Proof. By $\alpha > \gamma$ and $\alpha^2\gamma$, we get $\alpha > \frac{2}{3}\pi > \gamma$. Lemma 2.3 implies that $\alpha\beta\cdots$ is a vertex. As a consequence of Proposition 3.1 (see the remark), we have $\beta > \alpha > \gamma$. Combined with $\alpha > \frac{2}{3}\pi$, we have $\alpha + \beta + \gamma > 2\alpha + \gamma = 2\pi$, contradicting (2.5). \square

Proposition 3.3. *There is no dihedral tiling with vertex α^3 .*

Proof. If α^3 is a vertex, then we have $\alpha = \frac{2}{3}\pi$ and $\alpha^2\beta$ is not a vertex. Combined with $\beta > \alpha > \gamma$ and $\beta + \gamma > \pi$, we have $R(\beta^2) < \alpha, 2\gamma$. So $\beta^2\cdots = \beta^2\gamma$.

Suppose both $\alpha^3, \beta^2\gamma$ are vertices. We get

$$\alpha = \frac{2}{3}\pi, \quad \beta = \pi - \frac{1}{2}\gamma.$$

Substituting the above into (2.4), we get

$$\tan^2 \frac{1}{4}\gamma = 1 - \frac{2}{3}(4 \cos \frac{2}{5}\pi + 1) < 0,$$

a contradiction. Then $\beta^2\gamma$ is not a vertex. This further implies that $\beta^2\cdots$ is not a vertex.

By $\beta > \alpha > \gamma$ and $\alpha > \frac{3}{5}\pi$ and $\beta + \gamma > \pi$ and no $\beta^2\cdots$, we get $\beta\cdots = \beta\gamma^c, \alpha\beta\gamma^c$. Counting Lemma implies $\beta\cdots = \alpha\beta\gamma$, which is not a vertex, a contradiction. \square

Proposition 3.4. *The dihedral tiling with vertex β^3 is the fourth tiling in Figure 4.*

Proof. By β^3 , we get $\beta = \frac{2}{3}\pi$. Combined with $\alpha > \frac{3}{5}\pi$ and $\beta > \gamma$ and $\beta + \gamma > \pi$, we get the following,

$$\alpha > \frac{3}{5}\pi, \quad \beta = \frac{2}{3}\pi, \quad \gamma > \frac{1}{3}\pi.$$

Lemma 2.3 implies that $\alpha\beta\cdots$ is a vertex. The above inequalities imply $R(\alpha\beta) < \frac{11}{15}\pi < \alpha + \gamma, 3\gamma$. Meanwhile, by Proposition 3.1, we may assume no $\alpha\beta\gamma$. Combined with $\beta > \alpha > \gamma$ and β^3 , we get $\alpha\beta\cdots = \alpha\beta\gamma^2$. Then $\beta^3, \alpha\beta\gamma^2$ imply

$$\alpha + 2\gamma = \frac{4}{3}\pi, \quad \beta = \frac{2}{3}\pi.$$

Substituting the above into (2.4), we get

$$\alpha \approx 0.61881\pi, \quad \beta = \frac{2}{3}\pi, \quad \gamma \approx 0.35726\pi, \quad x \approx 0.12943\pi.$$

The above angle values determine all vertices. Hence we get

$$\text{AVC} = \{\beta^3, \alpha\beta\gamma^2\}. \tag{3.1}$$

From the above, we have $\alpha|\gamma\cdots = \alpha\beta\gamma^2$.

The arrangement of $\alpha|\gamma\cdots$ determines tiles T_1, T_2 in Figure 11. Then $\alpha_1\beta\cdots = \alpha\beta\gamma^c$ determines T_3 . Repeating the same argument we further determine T_4, T_5, T_6 . Hence $\alpha|\gamma\cdots = \beta|\alpha|\gamma\cdots = \alpha\beta\gamma^2$.

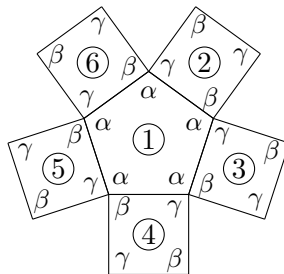


Figure 11: The arrangement of $\alpha|\gamma$

By $\alpha|\gamma\cdots = \beta|\alpha|\gamma\cdots = \alpha\beta\gamma^2$ around the pentagon and $\gamma|\gamma\cdots$ implying $\beta|\beta\cdots = \beta^3$, we therefore determine the fourth tiling in Figure 4. \square

Proposition 3.5. *There are three dihedral tilings with vertex $\alpha\beta^2$ in Figures 13, 16.*

Each of these tilings has 40 rhombi and 12 pentagons. They are the first three tilings of Figure 4.

Proof. By $\beta > \alpha > \gamma$ and $\alpha\beta^2$ and $\beta + \gamma > \pi$, we get $\pi > \beta > \frac{2}{3}\pi > \alpha > \frac{3}{5}\pi$ and $2\gamma > \alpha$. Then $\beta > \alpha > \frac{3}{5}\pi$ and $\alpha\beta^2$ imply $\frac{7}{10}\pi > \beta$. By $\alpha > \frac{3}{5}\pi$ and $2\gamma > \alpha$, we also get $\gamma > \frac{1}{2}\alpha > \frac{3}{10}\pi$. By $3\gamma > \frac{7}{10}\pi > \beta$ and $\alpha\beta^2$, we also have $3\alpha + \gamma, \alpha + \beta + 3\gamma > 2\pi$. This further implies that $\alpha^3\gamma\cdots$ is not a vertex and $\beta^2\cdots = \alpha\beta^2$ and $\alpha\beta\gamma\cdots = \alpha\beta\gamma^2$. We summarise the inequalities below,

$$\alpha > \frac{3}{5}\pi, \quad \beta > \frac{2}{3}\pi, \quad \gamma > \frac{3}{10}\pi.$$

Lemma 2.3 implies that $\alpha\gamma\cdots$ is a vertex. By the above inequalities and $\alpha\beta\gamma\cdots = \alpha\beta\gamma^2$ and no $\alpha^3\gamma\cdots$, we get $\alpha\gamma\cdots = \alpha^2\gamma^2, \alpha^2\gamma^3, \alpha\gamma^3, \alpha\gamma^4, \alpha\gamma^5, \alpha\beta\gamma^2$. Moreover, $\alpha\beta^2$ and one of $\alpha\gamma^3, \alpha\gamma^5, \alpha^2\gamma^3$ imply that there is no solution to (2.4) for $\alpha \in (\frac{3}{5}\pi, \frac{2}{3}\pi)$. So $\alpha\gamma^3, \alpha\gamma^5, \alpha^2\gamma^3$ is not a vertex. Hence we have

$$\alpha\gamma\cdots = \alpha^2\gamma^2, \alpha\gamma^4, \alpha\beta\gamma^2.$$

Any vertex above combined with $\alpha\beta^2$ uniquely determine angle values via (2.4) below

$$\begin{array}{lll} \alpha^2\gamma^2 : & \alpha \approx 0.63636\pi, & \beta \approx 0.68182\pi, & \gamma \approx 0.36364\pi. \\ \alpha\gamma^4/\alpha\beta\gamma^2 : & \alpha \approx 0.62526\pi, & \beta \approx 0.68737\pi, & \gamma \approx 0.34369\pi. \end{array}$$

Note that either one of $\alpha\gamma^4, \alpha\beta\gamma^2$ combined with $\alpha\beta^2$ yield the same angle values. The corresponding angle values above further imply that the vertices are one of the following combinations,

$$\begin{aligned} \text{AVC} &= \{\alpha\beta^2, \alpha^2\gamma^2\}; \\ \text{AVC} &= \{\alpha\beta^2, \alpha\gamma^4, \alpha\beta\gamma^2\}. \end{aligned}$$

We further divide the discussion into the cases below.

Case ($\text{AVC} = \{\alpha\beta^2, \alpha^2\gamma^2\}$). By $\text{AVC} = \{\alpha\beta^2, \alpha^2\gamma^2\}$, we know that $\gamma^3\cdots$ are not vertices and $\alpha\beta\cdots = \alpha\beta^2$ and $\alpha^2\cdots = \alpha\gamma\cdots = \alpha^2\gamma^2$.

The arrangement of $\alpha|\alpha$ determines tiles T_1, T_2 in the first picture of Figure 12. Up to mirror symmetry, $\alpha^2\cdots = \alpha^2\gamma^2$ determines T_3, T_4 . Then $\alpha_2\beta_3\cdots, \alpha_2\beta_4\cdots = \alpha\beta^2$ determine T_5, T_6 respectively. This implies $\gamma_5|\alpha_2|\gamma_6$. It means that there is an $\alpha^2\gamma^2 = |\alpha|\gamma|\alpha|\gamma|$.

The angle arrangement $\alpha|\gamma|\alpha$ determines tiles T_1, T_2, T_3 in the second picture of Figure 12. Then $\alpha_1\beta_2\cdots, \alpha_3\beta_2\cdots = \alpha\beta^2$ determine T_4, T_5 . This implies $\gamma_2\gamma_4\gamma_5\cdots$, which is not a vertex, a contradiction. So $\alpha|\gamma|\alpha\cdots$ is not a vertex. So $\alpha|\alpha\cdots$ is also not a vertex. Hence $\alpha^2\gamma^2$ is not a vertex.

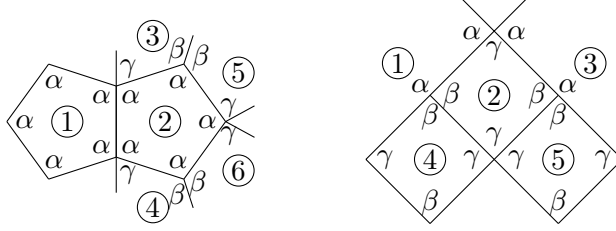


Figure 12: The arrangements of $\gamma|\gamma|\gamma$ and $\alpha|\gamma|\alpha$ and $\alpha|\alpha$

Case ($\text{AVC} = \{\alpha\beta^2, \alpha\gamma^4, \alpha\beta\gamma^2\}$). We have $\alpha\gamma\cdots = \alpha\gamma^4$ and $\alpha^2\gamma\cdots$ is not a vertex and $\beta^2\cdots = \alpha\beta^2$.

Reverse the deduction in the second picture of Figure 12, the angle arrangement of $\gamma|\gamma|\gamma$ leads to $\alpha_1\alpha_3\gamma_2\cdots$, a contradiction. Hence $\alpha\gamma^4$ is not a vertex. So $\alpha\gamma\cdots = \alpha\beta\gamma^2$.

The vertices $\alpha\beta^2, \alpha\beta\gamma^2$ imply

$$\beta = \pi - \frac{1}{2}\alpha, \quad \gamma = \frac{1}{2}\pi - \frac{1}{4}\alpha.$$

Substituting the above into (2.4), we get

$$\alpha \approx 0.62526\pi, \quad \beta \approx 0.68737\pi, \quad \gamma \approx 0.34369\pi, \quad x \approx 0.14901\pi.$$

With the above angle values and $\alpha\gamma\cdots = \alpha\beta\gamma^2$, one can determine all vertices satisfying (2.4). Hence we get

$$\text{AVC} = \{\alpha\beta^2, \alpha\beta\gamma^2\}.$$

Suppose there is one pentagon with five $|\alpha|\beta|\gamma|\gamma|$'s, then we determine the tiling in Figure 13.

Next, we assume that there is no pentagon with five $|\alpha|\beta|\gamma|\gamma|$'s. The same deduction in Figure 11 and no $\alpha^2\cdots$ show that any pentagon without five $|\alpha|\beta|\gamma|\gamma|$'s has at least one $\alpha\beta^2$. The unique angle arrangement of $\alpha\beta^2$ determines tiles T_1, T_2, T_3 in Figure 14. By mirror symmetry and no $\alpha^2\cdots$, we know that T_4 is a rhombus and we may assume T_4 with β_4, γ_4 as configured.

If there is another $\alpha\beta^2$, then $\alpha_1\beta_4\cdots = \alpha\beta^2$ determines T_5 in the first picture of Figure 14. The same argument also shows that T_6 is a rhombus. Then one of $\alpha_1\gamma_2\cdots, \alpha_1\gamma_4\cdots$ is $|\alpha|\beta|\gamma|\gamma|$.

If there is no more $\alpha\beta^2$, then $\alpha_1\beta_4\cdots = \alpha\beta\gamma^2$ determines T_5 in the second and third picture of Figure 14. As T_6 is a rhombus, the two angle configurations determine

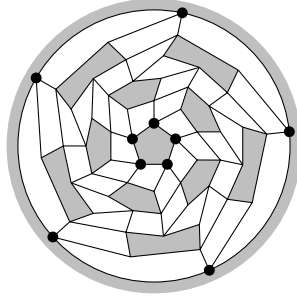


Figure 13: The tilings with $\alpha\beta^2, \alpha\beta\gamma^2$, where $|\alpha|\beta|\gamma|\gamma|$ denoted by a “•”

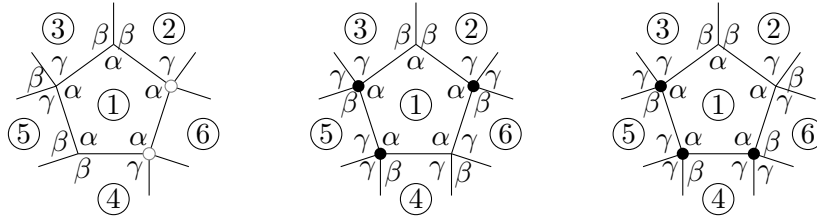


Figure 14: The five vertices at a pentagon with $\alpha\beta^2$

the tile in the second and the third picture respectively and we have exactly three $|\alpha|\beta|\gamma|\gamma|$'s in both pictures.

The second picture of Figure 14 can be translated into the first picture of Figure 15. We also know T_7, T_8 from $\alpha_1\beta_6\gamma_2\gamma_7$ and $\alpha_1\beta_5\gamma_3\gamma_8$ respectively. Then $\beta_2\beta_7\cdots, \beta_3\beta_8\cdots = \alpha\beta^2$ determine T_9, T_{10} , which implies $\gamma_2\gamma_3\cdots = \alpha\gamma^2$ or $\alpha^2\gamma^2\cdots$. None of them is a vertex. Hence the three $|\alpha|\beta|\gamma|\gamma|$'s at a pentagon must be consecutive.

If there is exactly one $|\alpha|\beta|\gamma|\gamma|$ at a pentagon, then by the symmetry of the first picture of Figure 14, we may assume $\alpha_1\gamma_2\cdots = |\alpha|\gamma|\beta|\gamma|$. Then focusing on T_1, T_2, T_3 , we translating the picture into Figure 15. Then $\alpha_1\beta_7\gamma_2\gamma_6, \alpha_1\beta_8\gamma_3\gamma_5$ determine T_7, T_8 . The mirror symmetry of T_1, T_2, T_3 and $\gamma_2\gamma_3\cdots = \alpha\beta\gamma^2$ determine T_9, T_{10} . This implies that T_{10} has at least two $|\alpha|\beta|\gamma|\gamma|$'s.

The above discussion entails that there is a pentagon with exactly three consecutive $|\alpha|\beta|\gamma|\gamma|$'s.

The vertices $\alpha\beta^2, \alpha\beta\gamma^2$ imply $\beta = 2\gamma$. Then every rhombus in the tilings can be subdivided into two equilateral triangles with three γ 's. This means that the underlying dihedral tiling is the snub dodecahedron. To obtain the remaining tilings, we merge the pairs of equilateral triangles in the snub dodecahedron by deleting their common edge in ways that there is a pentagon with exactly three $|\alpha|\beta|\gamma|\gamma|$'s.

In the snub dodecahedron in Figure 16, we denote the pentagons as P_1, P_2, \dots, P_{12} .

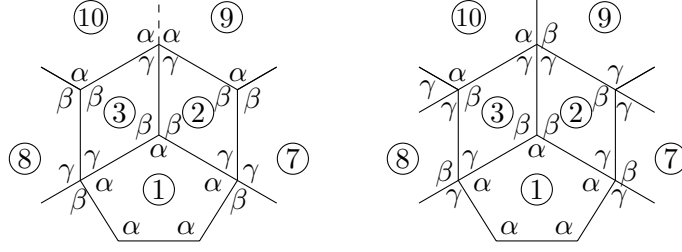


Figure 15: The arrangement of $\alpha\beta^2$

The edges e_i 's to be deleted are labeled by $i = 1, 2, \dots, 40$ in both pictures, so are the rhombus Q_1, Q_2, \dots, Q_{40} . Up to symmetry, we may assume that the central pentagon P_1 in Figure 16 has exactly three $|\alpha|\beta|\gamma|\gamma|$'s and we determine Q_1, Q_2, \dots, Q_6 . By $\alpha_4\beta_3\gamma_4 \cdots = \alpha\beta\gamma^2$, we further determine Q_7 . We repeat the same argument and determine Q_8, \dots, Q_{27} . Then P_{12} has two adjacent $|\alpha|\beta|\gamma|\gamma|$'s. This means that there is another $|\alpha|\beta|\gamma|\gamma|$ on either side of them. Suppose we have the third $|\alpha|\beta|\gamma|\gamma|$ in the first picture. Then we further determine Q_{28} . Repeat the same argument of $\alpha\beta\gamma \cdots = \alpha\beta\gamma^2$, we further determine Q_{29}, \dots, Q_{40} and obtain the tiling in the first picture. Suppose we have the third $|\alpha|\beta|\gamma|\gamma|$ in the second picture. Then we further determine Q_{28}, \dots, Q_{40} and obtain the tiling in the second picture.

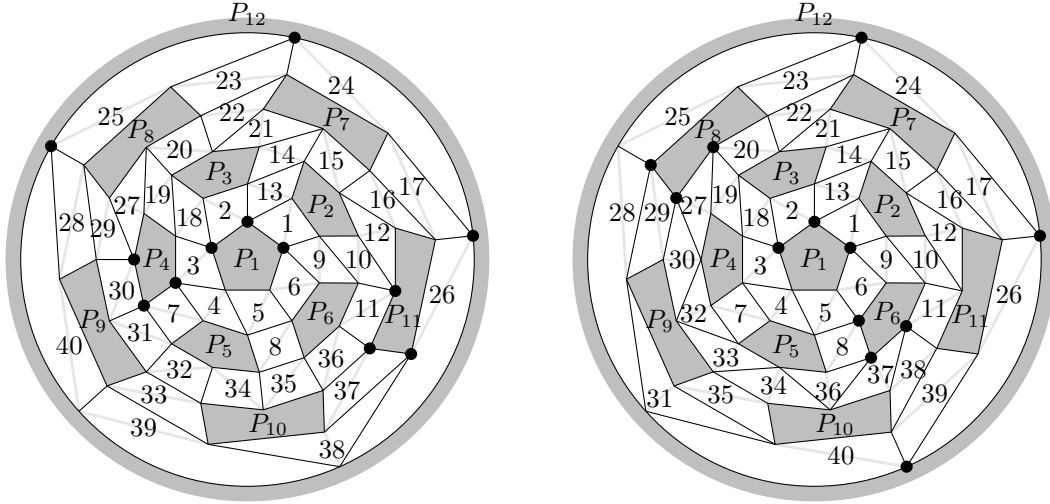


Figure 16: Dihedral tilings with $\alpha\beta^2, \alpha\beta\gamma^2$ and pentagons with exactly three vertices of angle arrangement $|\alpha|\beta|\gamma|\gamma|$, the trio $|\alpha|\beta|\gamma|\gamma|$'s are denoted by “●”

We sum up that the dihedral tilings with $\alpha\beta^2$ are the three tilings with underlying

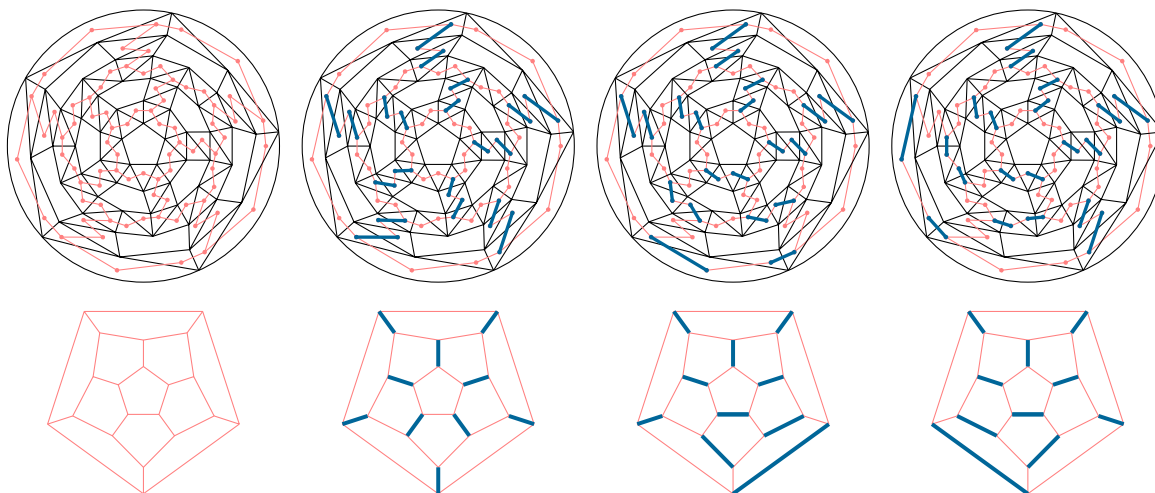


Figure 17: The correspondence between the dihedral tilings and the perfect matchings of the dodecahedron, “—————” and “—————” in the first row respectively corresponds to “—” and “—” in the second row

tiling of the snub dodecahedron as illustrated in the first picture of Figure 17. The underlying network with vertices at “the centre” of each triangle corresponds to the graph of the dodecahedron with each edge subdivided into three. As a quadrilateral is formed via deleting the common edge between two triangles, we highlight the adjacent pairs of such edges where the two non-adjacent end vertices of the “thick” edges have degree 3.

As seen in the second, third, and the fourth picture, such a pair uniquely corresponds to an edge of the dodecahedron and the collection of all such pairs form a perfect matching in the dodecahedron (see the second row). Note that an unmarked edges in the dodecahedron correspond to three consecutive edges in the network (two end vertices have degree 3) where the middle segment is to be deleted. This means that the three tilings can be derived from the perfect matching of the dodecahedron. \square

Proposition 3.6. *There is no dihedral tiling with vertex $\alpha^2\beta$.*

Proof. By Propositions 3.1, 3.3, 3.4, 3.5, we may assume that the only degree 3 vertices are $\alpha^2\beta, \beta^2\gamma$. Suppose both $\alpha^2\beta, \beta^2\gamma$ are vertices. By $\beta > \alpha > \gamma$ and $\alpha^2\beta$, we get $\beta > \frac{2}{3}\pi > \alpha$. Meanwhile, the two vertices imply

$$\beta = 2\pi - 2\alpha, \quad \gamma = 4\alpha - 2\pi.$$

Substituting the above into (2.4), one can show that there is no solution for $\alpha \in (0, \pi)$.

So $\alpha^2\beta$ being a vertex implies that $\beta^2\gamma$ is not a vertex. Combined with $\beta > \alpha > \gamma$ and the rhombus angle sum, we have $R(\beta^2) < R(\alpha\beta) = \alpha$ and $R(\beta^2) < 2\gamma$. Then $\beta^2 \dots$ is not a vertex. By no $\beta^2 \dots$, we also know that $\gamma|\gamma \dots$ is not a vertex. So $\gamma^c, \alpha\gamma^c, \beta\gamma^c$ are not vertices.

On the other hand, by $\alpha^2\beta$ and $\beta > \alpha > \gamma$, we get $\beta > \frac{2}{3}\pi > \alpha$. Then $\alpha > \frac{3}{5}\pi$ and $\beta > \frac{2}{3}\pi$ and no $\gamma^c, \alpha\gamma^c, \beta\gamma^c, \beta^2 \dots$ give the vertices

$$\text{AVC} = \{\alpha^2\beta, \alpha^3\gamma^c, \alpha^2\gamma^c, \alpha\beta\gamma^c\}.$$

By no $\gamma|\gamma \dots$, we have $\alpha^3\gamma^c = |\alpha|\alpha|\alpha|\gamma|, |\alpha|\alpha|\gamma|\alpha|\gamma|, |\alpha|\gamma|\alpha|\gamma|\alpha|\gamma| = \alpha^3\gamma, \alpha^3\gamma^2, \alpha^3\gamma^3$ and $\alpha^2\gamma^c = |\alpha|\gamma|\alpha|\gamma|$ and $\alpha\beta\gamma^c = |\alpha|\gamma|\beta|\gamma| = \alpha\beta\gamma^2$. Hence the AVC is updated as follows,

$$\text{AVC} = \{\alpha^2\beta, \alpha^3\gamma, \alpha^3\gamma^2, \alpha^3\gamma^3, \alpha^2\gamma^2, \alpha\beta\gamma^2\}.$$

Then we have $\alpha\gamma \dots = \alpha^3\gamma, \alpha^3\gamma^2, \alpha^3\gamma^3, \alpha^2\gamma^2, \alpha\beta\gamma^2$. Combining one of them with $\alpha^2\beta$, we get the angle formulae in terms of α . Substituting the angle formulae into (2.4), the only two vertices with solutions for $\alpha \in (\frac{3}{5}\pi, \frac{2}{3}\pi)$ are $\alpha^2\gamma^2, \alpha\beta\gamma^2$. By $\beta > \alpha > \gamma$, the vertices $\alpha^2\gamma^2, \alpha\beta\gamma^2$ are mutually exclusive. Hence we get the updated vertices below,

$$\begin{aligned} \text{AVC} &= \{\alpha^2\beta, \alpha^2\gamma^2\}; \\ \text{AVC} &= \{\alpha^2\beta, \alpha\beta\gamma^2\}. \end{aligned}$$

For both AVC's, by no $\gamma|\gamma \dots$, we have $\alpha^2\gamma^2 = |\alpha|\gamma|\alpha|\gamma|$ and $\alpha\beta\gamma^2 = |\alpha|\gamma|\beta|\gamma|$. It implies $\alpha|\alpha \dots, \alpha|\beta \dots = \alpha^2\beta$ and both $\alpha^2\gamma^2, \alpha\beta\gamma^2$ have angle arrangement $\gamma|\alpha|\gamma$.

The angle arrangement $\gamma|\alpha|\gamma$ determines tiles T_1, T_2, T_3 in Figure 18. Then $\alpha_2\beta_1 \dots = \alpha^2\beta$ determines the angles in T_4 . By mirror symmetry, we also get the angles in T_5 . By $\alpha_2|\alpha_4 \dots, \alpha_2|\alpha_5 \dots = \alpha^2\beta$, we get two adjacent β 's in T_6 , a contradiction.

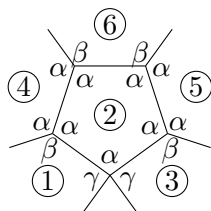


Figure 18: The angle arrangement $\gamma|\alpha|\gamma$

Hence there is no dihedral tiling for $\text{AVC} = \{\alpha^2\beta, \alpha^2\gamma^2\}, \{\alpha^2\beta, \alpha\beta\gamma^2\}$. □

Proposition 3.7. *The infinite family of dihedral tilings with vertex $\beta^2\gamma$ is in Figure 20.*

Each member of the infinite family has 2 pentagons and $4(2c - 1)$ rhombi, where $c \geq 2$ is the number of γ 's in the vertex $\alpha\beta\gamma^c$. They are illustrated in Figure 2.

Proof. By Proposition 3.6, we know that $\alpha^2\beta$ is not a vertex. As γ is the smallest angle, by $\beta^2\gamma$ we get $\beta^2\cdots = \beta^2\gamma$ and $\beta > \frac{2}{3}\pi$. By $\alpha > \frac{3}{5}\pi$ and $\beta > \frac{2}{3}\pi$ and $\beta > \alpha > \gamma$, we get all the vertices below,

$$\text{AVC} = \{\beta^2\gamma, \gamma^c, \alpha^{a \leq 3}\gamma^c, \beta\gamma^c, \alpha\beta\gamma^c\}. \quad (3.2)$$

From the above, we know that $\alpha^2\beta\cdots$ is not a vertex and $\alpha\beta\cdots = \alpha\beta\gamma^c$. Lemma 2.3 implies that $\alpha\beta\gamma^c$ is a vertex.

We will first show that $\gamma^c, \alpha^a\gamma^c$ are not vertices for dihedral tilings.

By $\alpha\beta\cdots = \alpha\beta\gamma^c$, the same deduction on $\alpha|\gamma\cdots$ in Figure 11 determines $\alpha|\gamma\cdots = \beta|\alpha|\gamma\cdots = \alpha\beta\gamma^c$. By $\alpha|\gamma\cdots = \beta|\alpha|\gamma\cdots$, we further know that $\alpha^a\gamma^c$ is not a vertex.

If γ^c is a vertex, then by $\beta^2\cdots = \beta^2\gamma$, the angle arrangement $\gamma|\gamma$ determines three tiles as illustrated in Figure 19. This process continues at γ^c and we determine a monohedral earth map tiling for each fixed $c \geq 3$. Further details about the earth map tilings can be seen in [8]. Hence γ^c is not a vertex for dihedral tilings.

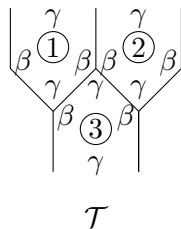


Figure 19: A timezone given by T_1, T_3 and $\mathcal{T} = c - \frac{1}{2}$ timezones, $c = 2$

For $c \geq 2$, we use \mathcal{T} to denote a block of $c - \frac{1}{2}$ timezones which consist of $c - 1$ timezones and one extra tile. Examples with $c = 2, 3$ are illustrated in Figure 19 and the first picture of Figure 2 respectively.

By no $\gamma^c, \alpha^a\gamma^c$, we get

$$\text{AVC} = \{\beta^2\gamma, \beta\gamma^c, \alpha\beta\gamma^c\}. \quad (3.3)$$

Since α appears at some vertex, we know that $\alpha\beta\gamma^c$ is a vertex. By the deduction in Figure 11, we get the central square in Figure 20. For any fixed $c \geq 2$, we can fill the

remaining γ 's of $\alpha\beta\gamma^c$ at the vertices $\alpha_1\beta_2\gamma_3 \cdots, \alpha_1\beta_3\gamma_4 \cdots, \alpha_1\beta_4\gamma_5 \cdots, \alpha_1\beta_5\gamma_6 \cdots, \alpha_1\beta_6\gamma_2 \cdots$ of Figure 11. Then the γ^c -part of each $\alpha\beta\gamma^c$ determine \mathcal{T} in Figure 20. The tiling is then completed by another square in the exterior of the “circular boundary” in Figure 20.

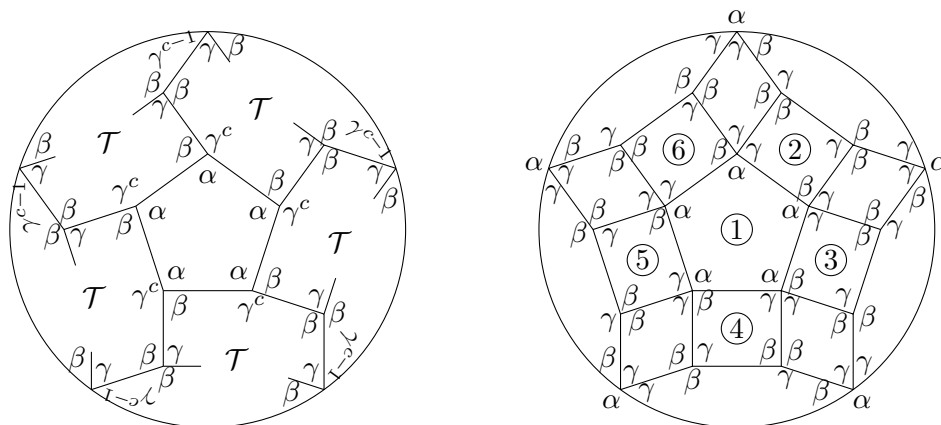


Figure 20: The infinite family of tilings with $\beta^2\gamma, \alpha\beta\gamma^c$

For $c = 2$, we illustrate the minimal member of the family in the second picture of Figure 20.

Geometric Realisation

Lastly, we show the geometric existence of these tilings. By $\beta^2\gamma, \alpha\beta\gamma^c$, we have

$$\alpha = \pi - (c - \frac{1}{2})\gamma, \quad \beta = \pi - \frac{1}{2}\gamma. \quad (3.4)$$

The geometric existence of the tilings means $\pi > \beta > \alpha > \frac{3}{5}\pi > \gamma$ and (2.4) is satisfied and $0 < \cos x < 1$. By the second identity of (3.4), the right hand side of (2.4) gives $\cos x = \frac{1}{2}(1 - \tan^2 \frac{1}{4}\gamma) \in (0, 1)$ for $\gamma \in (0, \pi)$. It suffices to check the first two conditions.

By $\gamma > 0$ and $c \geq 2$ and (3.4), we have $\beta > \alpha$. Meanwhile, for $\alpha = \alpha(\gamma) \in (0, \pi)$, by the second equation in (3.4) and (2.4) we get

$$\alpha(\gamma) = 2 \sin^{-1} \frac{2 \cos \frac{1}{5}\pi}{(3 - \tan^2 \frac{1}{4}\gamma)^{\frac{1}{2}}}.$$

Then by the first equation of (3.4), we get

$$c = c(\gamma) = \frac{1}{\gamma}(\pi - \alpha(\gamma)) + \frac{1}{2}. \quad (3.5)$$

For $\alpha > \frac{3}{5}\pi$ and $c \geq 2$, the first equation of (3.4) also implies $\gamma \in (0, \frac{2}{5}\pi)$. The inequality $\alpha(\gamma) > \frac{3}{5}\pi$ is equivalent to

$$\sin^{-1} \frac{2 \cos \frac{1}{5}\pi}{(3 - \tan^2 \frac{1}{4}\gamma)^{\frac{1}{2}}} > \frac{3}{10}\pi.$$

As $\sin \theta$ is strictly increasing on $(0, \frac{1}{2}\pi)$ and $\cos \frac{1}{5}\pi = \sin \frac{3}{10}\pi = \frac{1}{4}(1 + \sqrt{5})$, it is equivalent to $2 > (3 - \tan^2 \frac{1}{4}\gamma)^{\frac{1}{2}}$, which is true for $\gamma \in (0, \pi)$. Hence we always have $\alpha(\gamma) > \gamma$.

It remains to show that, for any integer $c \geq 2$, there is a $\gamma_c \in (0, \frac{2}{5}\pi)$ satisfying $c(\gamma_c) = c$. One can show that (3.5) is continuous and decreasing on $(0, \frac{2}{5}\pi)$ and $c(\frac{2}{5}\pi) = 1 < 2$ and

$$\lim_{\gamma \rightarrow 0^+} c(\gamma) = +\infty.$$

Then Intermediate Value Theorem implies that the desired γ_c exists and is unique.

Therefore we conclude that the infinite family of tilings in Figure 20 exist. \square

4 Tilings by Rhombi and m -gons with $m \geq 6$

Proposition 4.1. *There is no dihedral tiling with angle sum $2\beta + \gamma = 2\pi$ for $m \geq 6$.*

Proof. By $2\beta + \gamma = 2\pi$, we get

$$\beta = \pi - \frac{1}{2}\gamma.$$

Substituting the above into (2.4), we get

$$\cos x = \frac{1}{2}(1 - \tan^2 \frac{1}{4}\gamma). \quad (4.1)$$

An m -gon with maximum perimeter is the circumference. By $\alpha < \pi$ and $m \geq 6$, this implies $x < \frac{2}{m}\pi \leq \frac{1}{3}\pi$. Since $\cos \theta$ is strictly decreasing on $(0, \frac{1}{2}\pi)$, we further get $\cos x > \cos \frac{2}{m}\pi$. Combined with (4.1), we get

$$\frac{1}{2} > \frac{1}{2}(1 - \tan^2 \frac{1}{4}\gamma) > \cos \frac{2}{m}\pi,$$

which implies $m < 6$, a contradiction. Hence there is no tiling. \square

Proposition 4.2. *There is no dihedral tiling with vertex $\alpha^2\gamma$ for $m \geq 6$.*

Proof. By $\alpha^2\gamma$, we have $\alpha < \pi$ and $\alpha + \gamma > \pi$. Then $\alpha + \gamma, \beta + \gamma > \pi$ implies $R(\alpha\beta) < 2\gamma$. By $\alpha, \beta > \gamma$, we get $\alpha\beta\cdots = \alpha\beta\gamma$. Lemma 2.3 implies that $\alpha\beta\cdots = \alpha\beta\gamma$ is a vertex. Then $\alpha^2\gamma, \alpha\beta\gamma$ implies $\alpha = \beta$. Hence we have $2\beta + \gamma$. Therefore Proposition 4.1 implies that there is no dihedral tiling. \square

Proposition 4.3. *The dihedral tilings with vertex $\alpha\beta\gamma$ and $m \geq 6$ are in Figure 21.*

Proof. By $\beta + \gamma > \pi$, we get $R(\beta^2) < 2\gamma$. Then $\alpha, \beta > \gamma$ implies $\beta^2\cdots = \alpha\beta^2, \beta^3, \beta^2\gamma$. By (2.7), we know that $\alpha\beta^2, \beta^3$ are not vertices and by Proposition 4.1 we also know that $\beta^2\gamma$ is not a vertex. Hence $\beta^2\cdots$ is not a vertex.

By no $\beta^2\cdots$, we know that $\gamma|\gamma\cdots$ is not a vertex. Then $\beta\gamma^c$ is not a vertex. By $\alpha\beta\gamma$ and no $\beta^2\cdots, \beta\gamma^c$, we get $\beta\cdots = \beta\gamma\cdots = \alpha\beta\gamma\cdots = \alpha\beta\gamma$. Counting Lemma implies $\gamma\cdots = \alpha\beta\gamma$. So the other vertices consist of only α 's. For $m \geq 6$, we have $\alpha > (1 - \frac{2}{m})\pi \geq \frac{2}{3}\pi$ and α^a is not a vertex. Hence we have the vertices below,

$$\text{AVC} = \{\alpha\beta\gamma\}.$$

Starting at an $\alpha\beta\gamma$, by $\alpha\beta\cdots = \alpha\gamma\cdots = \beta\gamma\cdots = \alpha\beta\gamma$ we determine a tiling in the first picture of Figure 21. The tiling for $m = 6$ is given in the second picture.

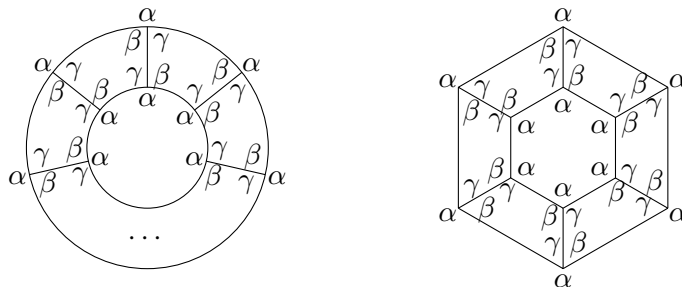


Figure 21: The dihedral tilings by rhombi and m -gon ($m \geq 6$) with $\alpha\beta\gamma$

The existence of these tilings has been discussed in the Geometric Realisation of Proposition 3.1. \square

References

- [1] C. P. Avelino, A. F. Santos: Spherical f-tilings by scalene triangles and isosceles trapezoids, I. *European Journal of Combinatorics*, 30(5):1221–1244, 2009.

- [2] Y. Akama, E. X. Wang, M. Yan: Tilings of the sphere by congruent pentagons III: edge combination a^5 . *Adv. in Math.*, <https://doi.org/10.1016/j.aim.2021.107881>, arXiv:1805.07217, 2021.
- [3] Y. Akama, M. Yan: On deformed dodecahedron tiling. *preprint*, arXiv:1403.6907, 2014.
- [4] A. M. Breda, P. S. Ribeiro: Spherical f-tilings by two non congruent classes of isosceles triangles - I. *Mathematical Communications*, 17:127–149, 2012.
- [5] A. M. Breda, A. F. Santos: Dihedral f-tilings of the sphere by rhombi and triangles. *Discrete Mathematics and Theoretical Computer Science*, 7:123–142, 2005.
- [6] A. M. Breda, P. S. Ribeiro, A. F. Santos: A class of spherical dihedral f-tilings. *European Journal of Combinatorics*, 30(1):119–132.
- [7] H. M. Cheung, H. P. Luk: Tilings of the sphere by congruent quadrilaterals with exactly two equal edges. *preprint*, arXiv:2108.06574, 2021.
- [8] H. M. Cheung, H. P. Luk, M. Yan: Tilings of the sphere by congruent quadrilaterals or triangles. *preprint*, arXiv:2204.02736, 2022.
- [9] H. M. Cheung, H. P. Luk, M. Yan: Tilings of the sphere by congruent pentagons IV: edge combination a^4b . *preprint*, arXiv:2307.11453, 2023.
- [10] H. H. Gao, N. Shi, M. Yan: Spherical tiling by 12 congruent pentagons. *J. Combinatorial Theory Ser. A*, 120(4):744–776, 2013.
- [11] H. P. Luk: Dihedral tilings of the sphere by regular polygons and quadrilaterals I: quadrilaterals with equal opposite edges. *preprint*, 2023.
- [12] H. P. Luk: Dihedral tilings of the sphere by regular polygons and quadrilaterals I: squares and rhombi. *preprint*, 2023.
- [13] D. M. Y. Sommerville. Division of space by congruent triangles and tetrahedra. *Proc. Royal Soc. Edinburgh*, 43: 85–116, 1922-3.
- [14] I. Todhunter. *Spherical Trigonometry*. MacMillan, 1886.
- [15] Y. Ueno, Y. Agaoka. Classification of tilings of the 2-dimensional sphere by congruent triangles. *Hiroshima Math. J.*, 32(3): 463–540, 2002.

- [16] E. X. Wang, M. Yan. Tilings of sphere by congruent pentagons I: edge combinations a^2b^2c and a^3bc . *Adv. in Math.*, <https://doi.org/10.1016/j.aim.2021.107866>, arXiv: 1804.03770, 2021.
- [17] E. X. Wang, M. Yan. Tilings of sphere by congruent pentagons II: edge combination a^3b^2 . *Adv. in Math.*, <https://doi.org/10.1016/j.aim.2021.107867>, arXiv: 1903.02712, 2021.